

NONDESTRUCTIVE EVALUATION OF DAMAGE IN
POLYETHYLENE PIPES USING ULTRASONIC TESTING

By

SAID EL-HAWWAT

A dissertation submitted to the

School of Graduate Studies

Rutgers, the State University of New Jersey

In partial fulfillment of the requirements

For the degree of

Doctor of Philosophy

Graduate Program in Civil and Environmental Engineering

Written under the direction of

Hao Wang

And approved by

New Brunswick, New Jersey

October, 2024

ABSTRACT OF THE DISSERTATION

Nondestructive Evaluation of Damage in Polyethylene Pipes using Ultrasonic Testing

By SAID EL-HAWWAT

Dissertation Director:

Dr. Hao Wang

In pipelines for natural gas distribution, more than 50% of damage is caused by third-party interference, such as foundation loads, traffic loads, or rock impingement. The remainder of damage occurs due to the limitations of the pipe's material in its service environment, such as resistance to slow crack growth (SCG), rapid crack propagation (RCP), thermal-oxidative aging, and stress-corrosion cracking (SCC). Due to the cost of excavating, user inconvenience, and required expertise, it is difficult to detect the onset of crack nucleation and propagation using conventional methods such as routine visual inspections or the hydrostatic pressure test. Therefore, effective nondestructive evaluation (NDE) techniques are sought so that cracks may be efficiently detected long before they compromise the integrity and functionality of a pipe system. However, due to high levels of material damping in plastic media, ultrasonic guided wave testing (UGWT) on plastic pipes is significantly unexplored compared to steel pipes.

This study aims to develop a systemic guideline of using piezoelectric (PZT) transducers for actuating and sensing of ultrasonic guided waves (USGW) on polyethylene (PE) pipes to locate external or internal cracks and assess their severity. A series of tests are performed on PE pipe specimens, in which PZT arrays are configured in varying pitch-catch arrangements on the outer surface. UGWT is conducted to determine material properties in the pipe's pristine state. Damage is subsequently introduced using high RPM cutting tools, and stress-waves are transmitted. Responses at multiple sensors are examined for each

actuated pulse, and degree of signal strength decay is recorded. Subsequently, the pipe is numerically simulated, and input properties are fine-tuned until response signals match the results of the experimental tests. The conditions of the waveguide are controllably varied to incorporate crack damage of different lengths, depths, thicknesses, axial and circumferential locations, and orientations. As such, a synthetic database of signal response data is compiled and expanded. This data is analyzed for damage-sensitive features, which are subsequently used to develop damage detection algorithms, such as training and testing a machine learning (ML) model. To validate the detection analysis, the developed algorithms are run over sensed signal responses from the experiments. This database is used to develop damage classification algorithms, such as support vector machine (SVM) and convolutional neural network (CNN). These models are further updated with independent numerical and experimental cases. The results proved the ability of UGWT for NDE of PE pipe by sequentially locating cracks and quantifying the crack geometry.

ACKNOWLEDGEMENTS

I have deep gratitude for the people who've encouraged me and kept me focused as I worked diligently and made progress throughout the course of writing this dissertation. Firstly, I would like to acknowledge Dr. Hao Wang for his vision and guidance. I would also like to acknowledge Dr. Jay Shah for his expertise in the field and his contributions to the research effort, as his help was indispensable. I have great appreciation for the dissertation committee of Dr. Nenad Gucunski, Dr. Husam Najm, and our outside committee member, Dr. Raimondo Betti, for their time, feedback, and support. Other members of the research group including Dr. Lukai Gao and Dr. Jingnan Zhao provided good introductions to the many phases of this project, and I am truly grateful. Furthermore, I would like to thank the US Department of Transportation (DOT) Pipeline and Hazardous Materials Safety Administration (PHMSA) through Competitive Academic Agreement Program (CAAP) for their sponsorship. Finally, I would like to thank my parents, Mr. Mohammed El-Hawwat and Dr. Razan Obaisi, for their belief in me and continued support, as well as my siblings, Arwa El-Hawwat, Noor El-Hawwat, and Hamza El-Hawwat.

Table of Contents

Table of Contents	v
Table of Figures	ix
List of Tables.....	xiv
1. Introduction.....	1
1.1 Problem Statement.....	1
1.2 Research Objectives	3
1.3 Research Scope.....	4
1.4 Outline of the Research.....	5
2. Background.....	7
2.1 Damage in PE Pipes	7
2.1.1. External Cracks.....	8
2.1.2. Internal Cracks.....	10
2.2. Acoustoelasticity.....	15
2.2.1. Dispersion Principles	15
2.2.2. Bulk Wave Propagation	18
2.2.3. Oblique Incidence.....	21
2.2.4. Guided Wave Propagation in Cylindrical Waveguides.....	22
2.2.5. Attenuation.....	28
2.3. Literature Review of Ultrasonic Testing on Pipes	31
2.3.1. Versatility of Ultrasonic Testing for Measuring Integrity	32

2.3.2. Effect of Attenuation.....	33
2.3.3. Damage Sensitivity	33
2.3.4 Machine Learning Models for Condition Assessment.....	37
3. Experimental Study.....	42
3.1 External Damage	42
3.1.1 Ultrasonic Testing Setup.....	42
3.1.2 Selecting Inspection Parameters	44
3.1.3 Circumferential Location of Damage.....	49
3.1.3 Quantification of Damage.....	50
3.2 Internal Damage	52
3.2.1 Selecting Inspection Parameters	55
3.2.2 Triangulation using Probabilistic Imaging.....	57
4. Numerical Modeling.....	64
4.1 External Crack.....	64
4.1.1 Estimation of Properties of PE Pipe.....	65
4.1.2 Circumferential Location of Damage.....	67
4.1.3 Quantification of Damage and Cross-Correlation Analysis.....	68
4.2 Internal Crack	72
4.2.1 Attenuation Study.....	73
4.2.2 Quantification of Damage and Cross-Correlation Analysis.....	75
4.2.3 Triangulation using Probabilistic Imaging.....	76

5.	Developing a Classification Algorithm for Condition Assessment of External Surface.....	83
5.1	Basics of Classification Algorithms.....	83
5.1.1.	Feature Selection.....	84
5.1.2.	Support Vector Machines (SVM).....	85
5.1.3.	Convolutional Neural Networks (CNN).....	87
5.2	Synthetic Database.....	88
5.3	SVM Based Model for External Pipe Damage.....	93
5.3.1	Signal Features in the Time, Frequency, and Time-Frequency Domains.....	94
5.3.2	Selection of Significant Features.....	98
5.3.3	Ring Focusing Method.....	99
5.3.4	Normalized Frequency Domain Features.....	100
5.3.5	Classification with SVM.....	101
5.3.6	Validation of Model using Numerical Test Cases.....	103
5.3.7	Validation of Model using Experimental Test Cases.....	105
5.4	CNN Based Model for Internal Pipe Damage.....	107
5.4.1	Generation of Continuous Wavelet Transforms (CWTs).....	108
5.4.2	Model Components.....	109
5.4.3	Quantification of Crack Geometry.....	111
5.4.4	Model Validation with Experimental Data.....	115
5.5	Models for Internal Damage with Increased Geometric Variability.....	116
5.5.1	SVM Model Development and Testing.....	118

5.5.2 CNN Model Development and Testing.....	122
6 Conclusions and Future Work.....	128
6.1 Conclusions	128
6.2 Future Work.....	130
References.....	133

PREVIEW

Table of Figures

Figure 1: Long-term Creep Rupture Behavior in PE Pipes [112]	8
Figure 2: External Crack from Long-term Third-Party Stress [76]	9
Figure 3: Microscopic View of Ductile Failure [67].....	10
Figure 4: Ductile Failure Resulting from Stress Rupture Test [76]	11
Figure 5: Brittle Through Thickness Crack Which Led to Leakage [76]	12
Figure 6: Crack Opening Mechanism during SCG [21]	14
Figure 7: Schematic for Progressive Crack Geometry.....	14
Figure 8: Wave Propagation.....	16
Figure 9: Nondispersive Wave (left), Dispersive Wave (Right) [87].....	17
Figure 10: Dispersion Curve for Phase Velocity (left) and Group Velocity (right) in an Aluminum Free Plate of 1 mm Depth [33].....	18
Figure 11: Normal Beam Incidence	21
Figure 12: Geometry and Boundaries for the One-Dimensional Cylinder Problem [87]	23
Figure 13: Directions of Wave Propagation and Particle Displacement in Modes of Longitudinally Advancing Wavefronts.....	24
Figure 14: The $L(0,3)$ Mode.....	24
Figure 15: Dispersion Curve for Phase Velocity (left) and Group Velocity (right) in a 3" Diameter, 10 mm Thick HDPE Pipe [64].....	25
Figure 16: Directions of Wave Propagation and Particle Displacement in Modes of Circumferentially Advancing Wavefronts.....	27
Figure 17: CSH Dispersion Curves for (a) Phase Velocity and (b) Group Velocity for a Pipe with an Aspect Ratio of 0.984, (c) Phase Velocity, and (D) Gropu Velocity for a Pipie with an Aspect Ratio of 0.5 [87].....	28
Figure 18: Stress - Strain Curve During Loading and Unloading in the Elastic Region	29

Figure 19: Phase Angle Form of Elastic	30
Figure 20: Attenuation Dispersion Curve for a Viscoelastic Plate [16]	31
Figure 21: Confusion Matrix for 100 dB Noise over USGW Application on a Steel Plate [115]	38
Figure 22: Classification Matrix for CNN Results over Corrosion Data in Simulated Carbon-Steel Pipes [75].....	41
Figure 23: Experimental Apparatus Diagram - Condition Assessment for External Damage	44
Figure 24: Phase Velocity Dispersion Curve of the Pipe Specimen.....	45
Figure 25: (a) Group Velocity and (b) Attenuation Curves of the Pipe Specimen	46
Figure 26: Transmitted Signals at (a) 35 kHz and (b) 50 kHz, Respectively	47
Figure 27: Experimental Signal Transmission Obtained at Different Propagation Distances for (a) $L(0,3)$ and (b) $L(0,4)$ Mode in Pristine Condition.....	48
Figure 28: Experimental Time Domain Peak Amplitude vs Axis for (left) $L(0,3)$ and (right) $L(0,4)$ Mode Response	50
Figure 29: Time Domain for the Experimental $L(0,3)$ Mode of Crack Length (a) 30 mm, (b) 45 mm and the $L(0,4)$ Mode of Crack Length (c) 30 mm, (d) 45 mm	52
Figure 30: Experimental Apparatus Diagram – Condition Assessment for Internal Damage.....	53
Figure 31: Pristine State Responses for Pulse Excitations of (a) 35 kHz (b) 50 kHz (c) 65 kHz	54
Figure 32: Transmission Index for Progressive Crack Growth.....	56
Figure 33: Experimental Signal Transmission Obtained at Different Propagation Distances in the Pristine State	57
Figure 34: Experimental Apparatus Diagram - Condition Assessment for Internal Damage	58
Figure 35: Probability of Damage at Individual Sensing Paths	59
Figure 36: Experimental Setup for Imaging via Triangulation of Crack (a) Cross-Sectional View (b) Side View	60
Figure 37: Schematic for Progressive Crack Geometry.....	61

Figure 38: Experimental Sensed Signal Responses for all Internal Damaged States at (a) Sensor 1, (b) Sensor 2, and (c) Sensor 3.....	62
Figure 39: Imaging through Ultrasonic Triangulation over Physical Internally Damaged Pipe.....	63
Figure 40: Numerical Model.....	65
Figure 41: Comparison of Signal Decays from Numerical and Experimental Attenuation Behavior for (a) $L(0,3)$ and (b) $L(0,4)$ Modes.....	66
Figure 42: Numerical Time Domain Peak Amplitude vs Axis for (left) $L(0,3)$ and (right) $L(0,4)$ Mode Response	67
Figure 43: Numerical Sensors Response at Axis 5 (a) $L(0,3)$ Mode Time Domain (b) $L(0,3)$ Mode Amplitudes (c) $L(0,4)$ Mode Time Domain (d) $L(0,4)$ Mode Amplitudes	70
Figure 44: Comparison of experimental and numerical signals (a) the $L(0,3)$, and (b) $L(0,4)$ mode at (30,30) crack geometry	71
Figure 45: Numerical Model Details	73
Figure 46: Numerical Signal Transmission Obtained at Different Propagation Distances for the $T(0,1)$ Mode in the Pristine Condition	74
Figure 47: Comparison of numerical and experimental attenuation behavior $T(0,1)$ Mode.....	75
Figure 48: Comparison of Transmission Index Relation with Crack Geometry between Experiment and Simulation.....	76
Figure 49: Illustration of the Finite Element Model	76
Figure 50: Numerically Sensed Signal Responses for all Damaged States at (a) Sensor 1, (b) Sensor 2, and (c) Sensor 3	78
Figure 51: Imaging through Ultrasonic Triangulation over Simulated Internally Damaged Pipe	80
Figure 52: Imaging through Ultrasonic Triangulation over Simulated Internally Damaged Pipe - Off Center Crack	82
Figure 53: Basic Structure of a Binary Class Confusion Matrix [28].....	84

Figure 54: Time Domain of L(0,3) and L(0,4) Mode Response under (left) 25 dB Noise and (right) 60 dB Noise	91
Figure 55: Analysis Procedure	93
Figure 56: Frequency Domain of all Simulated Signal Responses at Axes 4, 5, and 6	96
Figure 57: Relief-F Scores for all Features (a) $L(0,3)$ Mode, (b) $L(0,4)$ Mode.....	99
Figure 58: Normalized Frequency Domain Features vs Damaged State	101
Figure 59: SVM Hyperplanes for Central Frequency Features (Top) and Sum of Frequency Features (Bot).....	102
Figure 60: Normalized Frequency Domain Features for (37,22) (left) and (46,29) (right)	104
Figure 61: Normalized Frequency Domain Features for (40,30) (left) and (45,30) (right)	107
Figure 62: Deep Learning Flowchart.....	108
Figure 63: Magnitude Scalograms for Time-Frequency Domains of an Observation of State (a) (0,0), (b) (10,4), (c) (20,8), (d) (30,12), and (e) (40,16).....	109
Figure 64: Deep Learning Model Components.....	110
Figure 65: CNN Training	112
Figure 66: Confusion Matrix of Training Data	113
Figure 67: Confusion Matrix of Validation Check Data	114
Figure 68: Confusion Matrix of Testing Data	115
Figure 69: (l,d,t) Numerical Signal Responses - (top) Time Domains (bottom) Frequency Domains	118
Figure 70: (l,d,t) Numerical Signal Responses – Peak Amplitudes of Some Damaged States	119
Figure 71: Normalized Frequency Domain Features vs (l,d,t) Damaged State	119
Figure 72: (l,d,t) SVM Training Confusion Matrix	121
Figure 73: (l,d,t) SVM Testing Confusion Matrix	122
Figure 74: (l,d,t) CNN Model Training Accuracy and Loss	123
Figure 75: (l,d,t) CNN Model Training Confusion Matrix	124
Figure 76: (l,d,t) CNN Model Validation Confusion Matrix.....	124

Figure 77: (l,d,t) CNN Model Testing Confusion Matrix 125

PREVIEW

List of Tables

Table 1: Geometries and Materials in Literature	34
Table 2: Signal and Transducer Parameters in Literature	34
Table 3: Defect Geometry in Literature.....	35
Table 4: ASTM D2513 MDPE PE2708 Pipe Properties	42
Table 5: Ultrasonic Input Properties for Generating Dispersion Curves	44
Table 6: Dispersion Properties of Longitudinal Wave Modes.....	46
Table 7: External Crack Experimental Damaged States	50
Table 8: Damaged States for Internal Crack Experiment	56
Table 9: Experimental Damaged States - Condition Assessment for Internal Cracks.....	61
Table 10: PE Pipe Material Properties used in Numerical Simulation.....	66
Table 11: Cross-Correlation Coefficients between Experimental and Numerical Signals	72
Table 12: Numerical Damaged States	77
Table 13: Classes of External Crack Geometry for Machine Learning.....	89
Table 14: Classes of Internal Crack Geometry for Machine Learning.....	92
Table 15: Frequency Domain Features.....	97
Table 16: Frequency Bands at 7 th Level DWT	98
Table 17: Accuracy of Numerical Validation Classification.....	104
Table 18: Classification Accuracy of Simulated Cases – 25 dB Noise Level.....	105
Table 19: Accuracy of Experimental Validation Classification.....	106
Table 20: Classification of Experimental Signals using CNN Model.....	116
Table 21: Classes of Internal Crack Geometry for Machine Learning.....	116
Table 22: (l,d,t) Database Frequency Features	120
Table 23: Classification of New Numerical Data using (l,d,t) Models	125
Table 24: Classification of New Experimental Data using (l,d,t) Models.....	126

1. Introduction

1.1 Problem Statement

There are many material and labor advantages to using polyethylene (PE) in civil pipes, such as corrosion resistance, light weight [50], durability [14], high flexibility [80], ease of pipes connection [53], and reduced cost of installation [68]. As such, PE is ideal for utilities which transport fluids [6]. PE pipes have been used extensively in urban and suburban environments throughout the world since the 1970s and continue to exhibit good conditions even after decades of service [6]. Statistics from the United States DOT reveal that 97% of all plastic pipes in service as of 2006 comprise of PE [68]. High density polyethylene (HDPE) and medium density polyethylene (MDPE) are utilized in the distribution of natural gas [68].

Agencies face many challenges when dealing with PE pipes in service, as many factors contribute to infrastructure failure. Studies show that more than 50% of failures in PE pipes are caused by external loads such as excavation damage or rock impingement, which facilitate crack nucleation and growth on pipe external surfaces [68]. PE is more susceptible to damage from excavation loads than other pipe service materials due to its lower strength capacity. Puncture or penetration leads to leakage, which may be catastrophic [107]. Damage may also naturally occur externally through localized stresses from soil-structure interaction. Soil column weight, surcharge loads from traffic, and seasonal stress fluctuations from changing temperatures may also cause unanticipated external damage [49][91]. The remainder of failures occur internally due to fatigue cycles and pressure overload and may be categorized as slow crack growth

(SCG), ductile rupture (DR), and rapid crack propagation (RCP) [68]. In 2019 alone, utilities across the United States have spent over \$3 billion to replace more than 4,700 miles of pipeline [46].

Current infrastructure management solutions for PE pipes are reactive in nature and are met with many challenges. Visual examination of pipes is typically used to check joints immediately after welding [52]. This method is met with difficulty, as inspection effectiveness depends on the qualification of the personnel, and only obvious surface damages may be identified [117]. It's also unapplicable for detection of internal cracks. The hydrostatic pressure test is used to determine a pipe's hydrostatic strength, stress, or internal pressure leading to rupture [52]. However, this test is only effective if there are gross through-wall faults in the fusion joint, as visual bead verification is impossible for any crack that doesn't extend through to the external surface of its pipe [117][19]. Naturally, there has been a demand for technology which allows for proactive examination and management of pipeline infrastructure. Provided with such tools, utilities would progress past the current practice of reactive response to pipeline failures. Nondestructive evaluation (NDE) is an innovative solution which monitors the health of a structure without causing further damage. It provides a more accurate assessment than visual inspection and is more versatile than hydrostatic pressure testing [70].

Ultrasonic testing (UT) is an NDE method which has been used extensively in steel pipes [65][108][116] but has been neglected in PE pipes due to the effect of increased damping on ultrasonic attenuation [90][64]. It is ultrasonic guided wave (USGW) inspection through application of piezoelectric transducer (PZT) based signal generation. The electromechanical properties of PZT patches allow them to transmit user-defined signals onto any waveguide as stress waves. Upon traveling through a specified distance along the surface, the wave's response is distorted by imperfections and defects within the material. The micro-disturbances are converted back to electronic signals by sensors and recorded into a data-acquisition system. The ultrasonic response at the sensors may be observed in real time using an oscilloscope [9][78].

Ultrasonic modes in cylindrical waveguides disperse upon contact with discontinuities, such as cracks [41]. The influence of crack geometry on dispersion is complex and highly varied. To efficiently

apply this influence to NDE monitoring, numerical simulations and classification algorithms may be developed and studied. There are many benefits in the implementation of classification algorithms, such as: (1) Selection methods could effectively extract sensitive features for damage detection with less physical representation than mathematical models, (2) Features could provide better damage detection with minimized explicit formulation that physics-based methods rely on, and (3) Classification algorithms may incorporate structural uncertainties due to mixed data types and noise levels [115]. Classification is conventionally achieved through implementation of machine learning (ML) algorithms, such as the shallow-learning support vector machines (SVM) method or the deep-learning convolutional neural networks (CNN) method.

Numerous studies have successfully utilized such algorithms to classify damage in steel pipes. Lee *et al* were able to improve classification accuracy by implementing a Euclidean distance approach to better optimize the margins between the hyperplanes in the dimension of the dataset. For an application on long-range USGW over steel gas pipelines, it was determined that Euclidean SVM has a lower dependency on the conventional input parameters of the model than conventional SVM [57]. Shang *et al* developed a joint deep learning model using both CNN and Long Short-Term Memory (LSTM) algorithms, which accurately classified noisy signals. The complexity of the model was reduced through a principal component analysis (PCA) operation, improving the applicability [89]. However, due to complications in signal response from attenuation, there has been no study on classification of damage on PE pipes using classification algorithms.

1.2 Research Objectives

The main objective of this research is to develop an automated system for condition assessment of PE pipes using ultrasonic testing (UT), signal processing, imaging, and machine learning (ML) techniques. This is achieved through a two-step UT method which (1) detects an approximate location of any crack in a localized section of the pipe using actuating and sensing arrays and (2) automatically quantifies damage

severity using an ML model trained on numerous states of damage categorized by varying geometry. The details of the testing parameters in the second step will depend on the results in the first step. In testing for the damage developing in the likeliest service conditions, both internal and external crack damaged states are examined. Principles of stress-wave emissions naturally call for different procedures between external and internal crack detection. Thus, the intention of this research is for the two-step automated system to be deployed twice upon a routine NDE check of PE pipes: once for internal cracks and once for external cracks.

To facilitate a realistic framework for meeting this objective, certain limitations are imposed on the control variables in the problem. (1) the only damage type examined will be crack damage of varying geometries. As such, damage from environmental or chemical factors like stress-corrosion cracking will not be examined. (2) only a single crack will be applied to a localized region during experimental testing and simulation, as a fundamental analysis would require examination of basic damage. (3) The crack's location will be directly in the center, between actuating and sensing arrays.

These limitations will be referenced throughout this manuscript, as the service conditions of a PE pipe may limit the variety of challenges faced during its lifetime. Naturally, the primary task in developing an NDE method for condition assessment of PE pipes is to test for likeliest service conditions, which justifies these limitations. Future work may be undertaken to develop more robust models which may perform accurate condition assessment of pipes without the burden of these limitations.

1.3 Research Scope

To achieve the above objectives, the research work includes the following:

1. Selection of inspection parameters, using the commercial software, Graphic User Interface for Guided Ultrasonic Waves (GUIGUW) to compute the dispersion curves of different modes on a hollow cylindrical waveguide. The most damage-sensitive response modes are selected for the study.

2. Experimental testing on a pipe specimen, in which PZT transducers and ultrasonic testing equipment are properly calibrated and installed to generate and receive stress waves of different modes. Furthermore, material properties such as damping are studied, and signal wave responses to different types and levels of damage are recorded for analysis.
3. Numerical study, implemented by using Finite Element Analysis (FEA) through a commercial ABAQUS Standard, CAE and Explicit to simulate the pipe, damage, and stress wave propagation. The numerical study includes generating many hypothetical damage scenarios in which damage is simulated in the form of defects. Cracks are modeled variable by length, width, depth, axial and circumferential location, and orientation.
4. Damage detection, using such techniques as polar focusing and probability-based imaging to accurately determine the location of a crack on either the external or internal surfaces of the pipe.
5. Data processing, using additive gaussian white noise (AGWN) to populate a database by generating noisy signals based on the FEA response signals. The signals are transformed to other domains to thoroughly examine a wide range of features. Feature sensitivity algorithms are used to extract the most damage-sensitive features for input to develop ML models and other damage detection algorithms.
6. Validation, in which the developed automated system is checked for numerical and experimental data. The system is run over response signals pertaining to both newly simulated crack geometries in the finite element software and the experimental damaged states.

1.4 Outline of the Research

This dissertation is divided into seven chapters. The first chapter introduces the problem statement and research goals. Chapter two provides a background about types of failures in PE pipes, as well as USGW applications on hollow cylindrical media, reviewing previous research efforts in the field. Chapter 3 describes using ultrasonic testing in an experimental study for locating and quantifying damage, both on

the external and internal surfaces of PE pipes. Chapter 4 describes modeling a PE pipe in a finite element software for the purposes of simulated ultrasonic testing and gathering of synthetic data for analysis. Chapter 5 is devoted to the development of a classification algorithm for external surface damage in PE pipes, using both shallow learning and deep learning techniques. Finally, Chapter 6 provides a summary of this study, conclusions, and a work plan for future steps.

PREVIEW

2. Background

This chapter begins by describing damage in service PE pipes that have historically led to catastrophe and caused challenges for agencies. Next, this chapter will detail the scientific background related to the ultrasonic stress wave propagation in solid media. Finally, this chapter concludes with a literature review over previous studies which have implemented this science to examine signal responses to damage in pipes and other infrastructure.

2.1 Damage in PE Pipes

Despite the many material, chemical, and economic advantages of polyethylene in natural gas distribution systems, agencies face many challenges when dealing with PE pipes in service, as many factors may contribute to infrastructure failure. These challenges stem from inherent structural weaknesses in PE, specifically those relevant to lifetime integrity. When loaded by internal pressure P from fluid flow, the walls of a pipe sustain hoop stress σ_{hoop} according to (1)

$$\sigma_{hoop} = P \cdot \frac{d - s}{2s} \quad (1)$$

, in which d is the outer diameter of the pipe and s is the wall thickness [40]. Due to this long-term sustained stress, PE pipes in service naturally undergo stress-relaxation and creep behavior following a three-stage process. These stages are categorized by the leading causes of failure during pipe's lifetime. Stage I is dominated by ductile failure, stage II quasi-brittle failure, and stage III brittle failure [112]. The stages are identified by three distinct regions in the relation between σ_{hoop} and time to failure, t_f (**Figure 1**).

The mechanisms of failure in Stage I are initiated by ductile fractures, including both internal ductile rupture (DR) from pressure overload and external yielding from third-party damage. This region is characterized by high stress early in the pipe's lifespan. In Stage II, the dominant failure mode is slow-crack growth (SCG) caused by fatigue [68]. This failure mechanism is microscopically ductile and macroscopically brittle. In Stage III, the failure mode is purely brittle, and is a product of environmental aging [82].

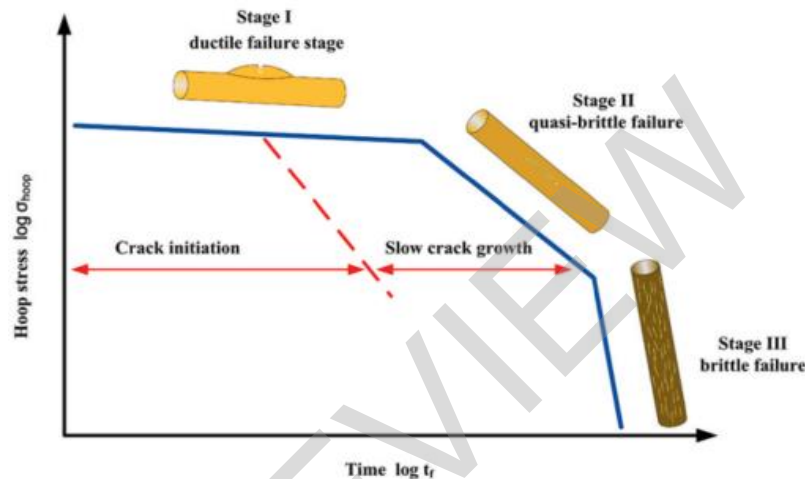


Figure 1: Long-term Creep Rupture Behavior in PE Pipes [112]

2.1.1. External Cracks

During Stage I, service pipes have experienced a relatively small number of fatigue cycles (**Figure 1**). Thus, they have a great capacity for hoop stress, and the chemical stability of the polyethylene polymer minimizes risk of degradation from environmental aging. Alternatively, external loads may occur at any point during the lifetime of the pipe. Therefore, third-party damage is the likeliest source of failure in this stage. The failure mechanism of this damage is ductile, which is characterized by massive yield of material in the vicinity of the over-loading [112]. The pipe in **Figure 2** exhibits a crack which was caused by a metal pipeline pressing against the plastic over time, generating long-term stress intensification. This crack caused a fatal natural gas explosion and fire in Lake Dallas, Texas, in August 1997.



Figure 2: External Crack from Long-term Third-Party Stress [76]

The other dominant type of failure in this stage, ductile rupture (DR) [13], is an internal failure mechanism which is a direct result of the practices of the servicing agency, as described in 2.1.2. Internal Cracks.

Ductile failure occurs when the polymer or pipe is loaded beyond its yield strength [55]. On a microscopic level, the long polymers which constitute polyethylene are typically held together by tie molecules. Tie molecules may be thought of as the “cement” which holds the lamellar “bricks” together. If tensile loads are applied normal to the face of the lamellae, the tie molecules are stretched as shown in **Figure 3**. During excessive loading, the molecules may no longer be stretched, and the molecular building blocks break up into smaller units. Macroscopically, ductile yielding from third party damage causes thinning and stretching in the localized region of overload [67].

At the microscopic level, the amorphous and crystalline regions of PE are connected via a polymer chain and reinforced with tie molecules. During heavy or long-lasting ductile load, the tie molecules are stretched until they can no longer support the applied stress. Subsequently, the microscopic structure breaks up into smaller units until it is strained to the point of complete molecular degradation [67].

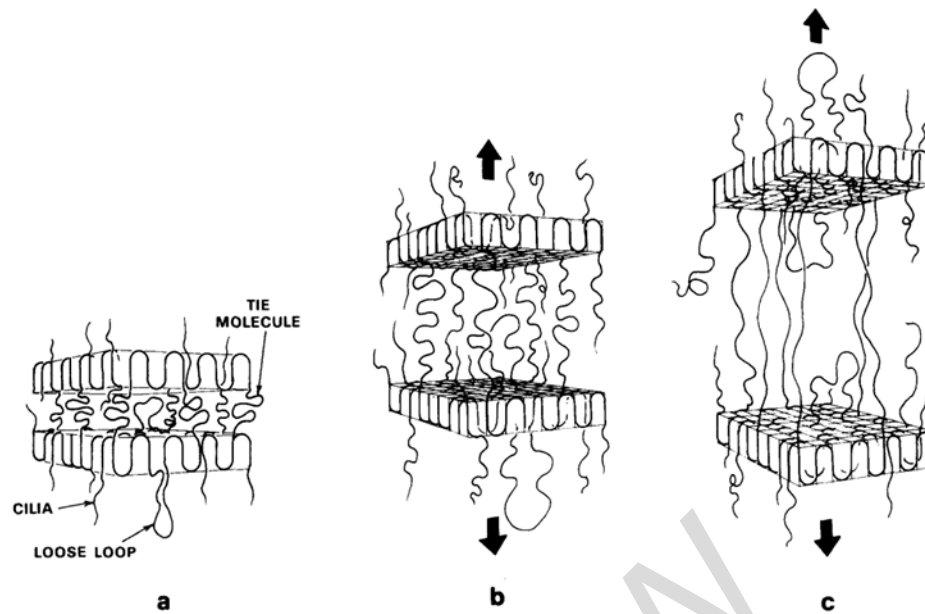


Figure 3: Microscopic View of Ductile Failure [67]

Due to the randomness of third part damage, external cracks are highly variable in their geometries. Conversely, certain attributes of internal cracks are more deterministic due to the usual failure mechanisms which lead to their nucleation.

2.1.2. Internal Cracks

Three types of failure mechanisms may occur during the lifetime of a plastic pipe which contribute to the nucleation and propagation of an internal crack: Ductile rupture (DR), slow-crack growth (SCG) and rapid crack propagation (RCP). DR is the simplest of these mechanisms, as it is caused by direct pressure overloads during operation. Over pressurization causes the pipe diameter to expand, resulting in the pipe wall thinning and stretching to the degree that the ligament is not suitable for resisting the induced large circumferential hoop stresses [68]. The time to ductile failure depends on creep rate, as habitual service pressures over capacity leads to large amounts of deformation [112]. DR is represented microscopically by **Figure 3** and macroscopically by **Figure 4**.